

DEVELOPMENT OF PULSED MULTIPOLE MAGNET FOR AICHI SR STORAGE RING*

K. Ito[#], M. Hosaka, A. Mano, T. Takano, Y. Takashima, Nagoya University, Nagoya, Japan
 N. Yamamoto, KEK, Tsukuba, Japan
 K. Hayashi, M. Katoh, UVSOR, Okazaki, Japan

Abstract

We designed a Pulsed Multipole Magnet (PMM) for Aichi SR storage ring. The design goal is to suppress displacement of stored electron beams smaller than 10 percent of stored beam size. In our past research, we established a technique to compensate magnetic field error. At this time, we estimated effects of magnetic field generated by current leads and of electric field caused by potential differences in the coil. Then, we designed the configuration of current leads to minimize the perturbations to the stored beam. It is expected that the amplitude of electron beam would be suppressed to 4 percent horizontally and 0.08 percent vertically of the beam size.

INTRODUCTION

Aichi SR, a 1.2 GeV storage ring light source, is the newest synchrotron light source in Japan. The ring is equipped with four superconducting bending magnet, which can provide hard X-rays to more than 10 beam-lines. The storage ring has been operated with the top-up injection mode since the beginning of the users operation in 2013[1]. The parameters of Aichi SR storage ring are shown in Table 1. So far, the stability of 0.2% for the stored beam current is achieved. In the usual injection scheme, four pulsed kicker magnets create a bump orbit. At the beam-lines in this orbit, synchrotron radiation is lost due to momentary displacement of a stored beam orbit. Because Aichi-SR is relatively small, the local bump lies in about a half of the circumference and there exist many beam-lines. For those reasons, this problem is quite essential.

In order to solve it, we decided to introduce the PMM injection scheme, which enables beam injection without

Table 1: Parameters of Storage Ring

Electron Energy	1.2 GeV
Circumference	72 m
Current	>300 mA
Natural emittance	52 nm-rad
Betatron tune	(4.72, 3.18)
RF frequency	499.7 MHz
Harmonics number	120
(β_{x1}, β_{y1}) @superbend	(1.63, 3.99) m
(β_{x2}, β_{y2}) @straight section	(29.9, 3.72) m
$(\sigma_{x1}, \sigma_{y1})$ @superbend	(0.328, 0.0909) mm
$(\sigma_{x2}, \sigma_{y2})$ @ straight section	(1.60, 0.0849) mm

[#] ito.keiia@j.mbox.nagoya-u.ac.jp

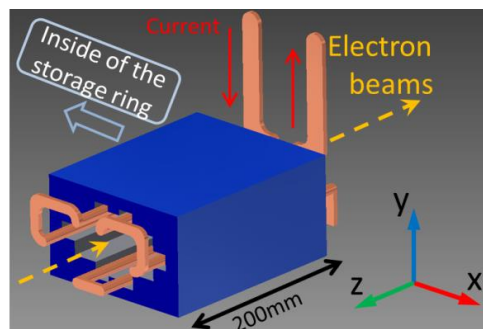


Figure 1: The appearance of the PMM of Aichi SR.

perturbing the stored beam [2,3,4,5]. However, in reality, a PMM didn't completely suppress perturbations to stored beams. The effect of quadrupole field was treated in [3] and the effect of dipole field error and its compensation method was discussed in [5]. In this work, we treat electric field generated by the conductors and magnetic field generated by current leads, which have not been considered in the previous studies, and design a PMM. Our design goal is suppressing the amplitude of the electron beam oscillation less than 10 percent of stored beam size.

PULSED MULTIPOLE MAGNET

Figure 1 shows the appearance of the PMM of Aichi SR. It consists of a yoke and a single-turn coil. The yoke is painted blue in Fig. 1 and is made of laminated silicon steel. Its height, width and length are 120 mm, 180 mm and 200 mm, respectively. Electron beams pass through this yoke. The coil is painted orange and as a matter of convenience, we divide it to 3 parts. First, we call the part inside of the yoke "main coils." Second, we call the part outside of the yoke in the left side of Fig. 1 "upstream current leads" and similarly, call the opposite side "downstream current leads." Pulsed current runs through the coil to excite the magnetic field. Its waveform is a half-sine pulse whose width is 960 ns. Figure 2 shows the cross-section of the PMM with magnetic field lines. The current runs through 6 conductors in alternate directions and excites sextupole magnet field. Figure 3 shows the magnetic field distribution in the horizontal plane. The stored beam passing at the center is not affected by the magnetic field. On the other hand, the injected beam passing at 20 mm from the center is kicked and captured. The $B_y \cdot L$ component of the magnetic field has to be about 27 mT · m at the injected beam orbit.

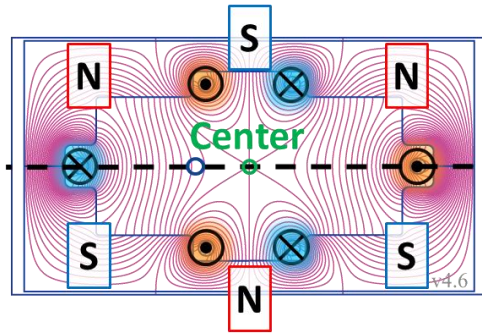


Figure 2: Cross-section of PMM.

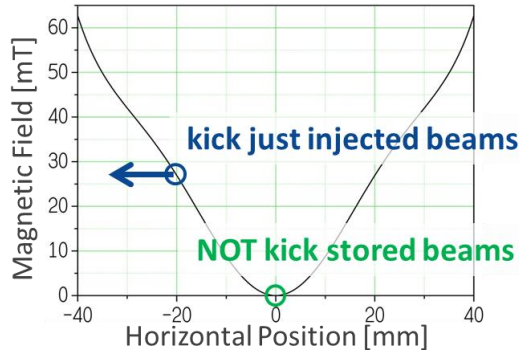


Figure 3: Magnetic field distribution in the horizontal plane.

FIELD OPTIMIZATION

Offset of Magnetic Field Center

The offset of the magnetic field center caused by manufacturing errors can be compensated by inserting some pieces made of magnetic substance into a PMM [5]. This method was established by us in a past study.

Electric Field in PMM

Electric field may arise in the PMM. This field may be generated by potential differences between six main coils when the pulsed current is running through the inductive coil.

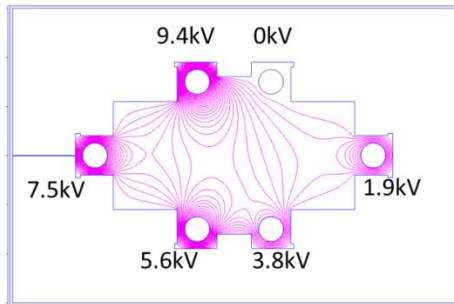


Figure 4: Potential and isoelectric lines in PMM.

Figure 4 shows isoelectric lines in PMM simulated by using POISSON code [6]. We estimated the electric field to be 7.44 kV in horizontal ($E_x \cdot L$) and 0.042 kV in vertical ($E_y \cdot L$) at the magnet center. The stored beam will be kicked by $-6.2 \mu\text{rad}$ horizontally (toward the inside of the storage ring) and by $-0.035 \mu\text{rad}$ vertically

by this field.

Here, we don't take into account the Ti-coating on the ceramic beam duct which may prevent the electric field from penetrating into the duct. Therefore we estimate in the worst case.

Magnetic Field Generated by Current Leads

The pulsed current running in the current leads also generates magnetic field. Instead of a 3D calculation, here we calculate this quasi-analytically. We divide current leads to simple straight parts and apply the Biot-Savart law for each part. Then, we have obtained the following expressions;

$$B_x = 0$$

$$B_y = \frac{\mu_0 I}{4\pi} \frac{z}{Y^2 + z^2} \left\{ \frac{X}{\sqrt{X^2 + Y^2 + z^2}} - \frac{X + L}{\sqrt{(X + L)^2 + Y^2 + z^2}} \right\}$$

$$B_z = \frac{\mu_0 I}{4\pi} \frac{Y}{Y^2 + z^2} \left\{ \frac{X}{\sqrt{X^2 + Y^2 + z^2}} - \frac{X + L}{\sqrt{(X + L)^2 + Y^2 + z^2}} \right\}$$

$$B_x = \frac{\mu_0 I}{4\pi} \frac{z}{X^2 + z^2} \left\{ \frac{Y + L}{\sqrt{X^2 + (Y + L)^2 + z^2}} - \frac{Y}{\sqrt{X^2 + Y^2 + z^2}} \right\}$$

$$B_y = 0$$

$$B_z = \frac{\mu_0 I}{4\pi} \frac{X}{X^2 + z^2} \left\{ \frac{Y + L}{\sqrt{X^2 + (Y + L)^2 + z^2}} - \frac{Y}{\sqrt{X^2 + Y^2 + z^2}} \right\}$$

The magnetic field produced by the horizontal (bars lying in the x-direction) parts are given by Eq. 1. The field produced by the vertical (bars lying in the y-direction) parts are given by Eq. 2. Here, z represents the z -coordinate at the observation point from a plane on which current leads lie. The observation point is on stored beam axis. L represents the length of the bar. For Eq. 1, X and Y represent x and y -coordinates at the left end of the bar. The forward direction of I is from left to right. For Eq. 2, X and Y represent the x and y -coordinates at the bottom end of the bar. The forward direction of I is from bottom to top. By summing up the contribution from each bar, we can calculate 3D magnetic field from current leads.

In reality, the magnetic field may be canceled partially by the eddy current in the yoke made of laminated silicon steel or a neighboring chamber made of stainless steel. In order to take their interference into account, we assume that magnetic flux can penetrate into the yoke from x and y -direction but not from z -direction. Moreover, we also assume that no magnetic flux can penetrate into the stainless part of the chamber. Then, we estimate the 3D magnetic field by combining analytical calculations and this 2D simulation.

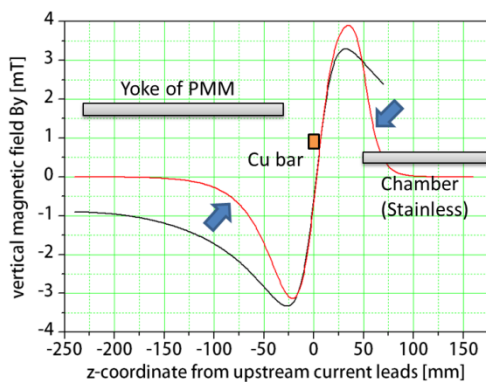


Figure 5: A shift of magnetic field distribution and arrangement around a current lead.

Field Optimization

The effect of the electric field doesn't depend on configurations of current leads because it is dominantly produced by the main coils inside of the yoke. Its kick direction is always toward inside of the storage ring. On the other hand, the kick direction by the magnetic field changes depending on the current lead configuration as follows (see Fig. 6).

- (1) At upstream current leads, the farther from the center we place upper bars, the more largely stored beams are kicked toward the outside of the storage ring.
- (2) At downstream current leads, as we place lower bars farther from the center, stored beams get kicked toward the outside. (As we keep lower bars on the simplest arrangement, stored beams are kicked toward the inside)

We can cancel the effects of the electric field from the main coils and the magnetic field from the current leads each other by optimizing the configuration of the current leads. We designed the configuration of the current leads (see Fig. 6). In Table 2, we compare the result of the optimization with the simple design. In this table, $\theta_{x,M}$

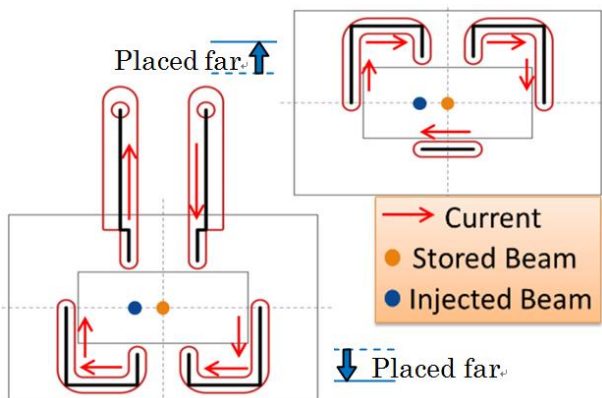


Figure 6: Design strategy for the current leads; upstream (top) and downstream (bottom).

We placed the upper bars at the upstream side and the lower bars at the downstream side as far from the center as possible and $\Delta\theta_{x,E}$ represent the horizontal kick angle by the magnetic field from the current leads and that by

the electric field, respectively. COD_x represents the maximum horizontal closed orbit distortion caused by the horizontal kick.

Table 2: Comparisons of Effects in Different Configurations

Configurations	Simple	Optimized
$B_y \cdot L [\mu T \cdot m]$	2.67	-7.77
$\Delta\theta_{x,M} [\mu rad]$	-0.7	1.9
$\Delta\theta_{x,M} + \Delta\theta_{x,E} [\mu rad]$	-6.2-0.7=-6.9	-6.2+1.9=-4.3
$COD_x [\mu m]$	104	65
$COD_x/\sigma_{x2} [\%]$	7	4

CONCLUSION

In this work, we designed the configuration of the current leads on the basis of the field estimation. It is expected that the amplitude of electron beam would be suppressed to 4 percent horizontally and 0.08 percent vertically of the beam size. Our design goal is suppressing it less than 10 percent.

Now, the PMM and its power supply have been already made and we will carry out magnetic field measurements in detail.

ACKNOWLEDGMENT

The authors are thankful to Prof. Y. Takeda, Director of Aichi synchrotron radiation center for supporting this work. We are also thankful to Mr. K. Takami for helpful discussions.

REFERENCES

- [1] N. Yamamoto, *et. al.*, *AIP*, **1234**, pp. 591-594 (2010).
- [2] N. Yamamoto, *et. al.*, *Proc. of IPAC 2014*, WEPRO011 (2014).
- [3] K. Harada, *et. al.*, *Phys. Rev. STAB* **10** (12) (2007) 123501.
- [4] H. Takaki, *et. al.*, *Phys. Rev. STAB* **13** (2010) 020705.
- [5] N. Yamamoto, *et. al.*, *NIM. A*, **767** (2014) 26-33.
- [6] Poisson/Superfish, Los Alamos National Laboratory Report No. LA-UR-96-1834.